

ON ITERATIVE SOURCE-CHANNEL DECODING FOR VARIABLE-LENGTH ENCODED MARKOV SOURCES USING A BIT-LEVEL TRELLIS

Ragnar Thobaben and Jörg Kliewer

University of Kiel
Institute for Circuits and Systems Theory
Kaiserstr. 2, 24143 Kiel, Germany
Phone: +49-431-880-6130, Fax: +49-431-880-6128
E-Mail: {rat, jkl}@tf.uni-kiel.de

ABSTRACT

In this paper we present a novel bit-level soft-input/soft-output decoding algorithm for variable-length encoded packetized Markov sources transmitted over wireless channels. An interesting feature of the proposed approach is that symbol-based source statistics in form of transition probabilities of the Markov source are exploited as a-priori information on a bit-level trellis. When additionally the variable-length encoded source data is protected by channel codes, an iterative source-channel decoding scheme can be obtained in the same way as for serially concatenated codes. Based on an extrinsic information transfer chart analysis of the iterative decoder computer simulations show for an AWGN channel that by using reversible variable-length codes with free distance greater than one in combination with rate-1 channel codes a reliable transmission is possible even for highly corrupted channels.

1. INTRODUCTION

In order to achieve a reliable transmission of sequences encoded with variable-length codes (VLCs) many authors have focused on joint source-channel decoding schemes based on a trellis representation of the variable-length encoded bit-stream. This allows to apply a soft-in/soft-out decoding approach and, in combination with channel codes, to utilize an iterative decoding scheme. For example, in [1] a symbol-level trellis representation for uncorrelated variable-length encoded data packets is presented, where the BCJR-algorithm [2] is used as a-posteriori probability (APP) decoder. This approach is extended in [3] to first-order Markov sources, where the residual source correlation is additionally exploited in the decoding process. On the other hand, a bit-level trellis is proposed in [4, 5]. This type of trellis has the advantage that the number of trellis states only depends on the VLC tree depth, and thus for increasing source packet lengths the complexity does not grow as for the symbol-level trellis. In [6] an iterative decoder for a variable-length encoded source being serially concatenated

with a turbo code is proposed by merging the bit-level trellis from [4] with the trellis for one constituent channel code.

In this paper we present a joint source-channel decoding approach for packetized variable-length encoded correlated source data based on the bit-level VLC trellis from [4]. As a novelty we show for a first-order Markov source that by using an appropriately adapted soft-input/soft-output decoder all source correlation can be exploited in the decoder with only a slight increase in complexity compared to the approach in [5]. When the resulting variable-length encoded bit-stream is additionally protected by a channel code the proposed bit-level VLC decoder can be used as constituent decoder in an iterative source-channel decoding scheme. A suitable channel code is then chosen via an extrinsic information transfer (EXIT) chart analysis [7]. We demonstrate that by allowing additional redundancy for the VLC in form of reversible variable-length codes (RVLCs) [8] with an increased Hamming distance between equal-length code-words good recursive systematic convolutional (RSC) channel codes with a just code rate of one and low memory can be found.

2. APP SOURCE DECODING

2.1. Transmission model

The derivation of the APP source decoder is based on the transmission system shown in Fig. 1, where a packet of K correlated source symbols is given by $\mathbf{U} = [U_1, U_2, \dots, U_K]$. A subsequent (vector-) quantization of source symbols U_k results in indices $I_k \in \mathcal{I}$ from the finite alphabet $\mathcal{I} = \{0, 1, \dots, 2^M - 1\}$ represented with M bits. Due to delay and complexity constraints for the quantization stage, a residual index correlation remains in the index vector \mathbf{I} , which is modeled as a first-order (stationary) Markov process with index transition probabilities $P(I_k = \lambda | I_{k-1} = \mu)$ for $\lambda, \mu \in \mathcal{I}$. The quantization stage is followed by a VLC encoder which maps a fixed-length index I_k to a variable-length bit vector $\mathbf{c}(\lambda) = \mathcal{C}(I_k = \lambda)$

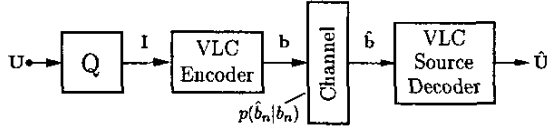


Fig. 1. Model of the transmission system

of length $l(\mathbf{c}(\lambda))$ using the VLC with the codetable \mathcal{C} . The output of the VLC encoder is given by the binary sequence $\mathbf{b} = [b_1, b_2, \dots, b_N]$ of length N where $b_n \in \{0, 1\}$ represents a single bit at bit index n . The transmission of one bit over the memoryless channel with the p.d.f. $p(\hat{b}_n | b_n)$ leads to a soft-bit $\hat{b}_n \in \mathbb{R}$ at the channel output.

2.2. Trellis representation

Since a VLC encoder can be seen as a finite state machine with binary output all possible output sequences \mathbf{b} can be described in a trellis diagram. A quite simple trellis representation is proposed in [4], where the VLC trellis is derived from the corresponding code tree by mapping each node to a specific trellis state. The root node and all leaf nodes are mapped to the same trellis state, since in a sequence of codewords every leaf becomes the root of the tree for the next codeword. Each transition from state S_{n-1} to state S_n is caused by a single bit $b_n \in \{0, 1\}$ at time instant $n = 1, \dots, N$ at the output of the VLC encoder. An example is given in Fig. 2, where the code tree and a trellis segment for the reversible variable-length code (RVLC)

$$\mathcal{C} = \{\mathbf{c}(0)=[11], \mathbf{c}(1)=[00], \mathbf{c}(2)=[101], \mathbf{c}(3)=[010], \mathbf{c}(4)=[1001], \mathbf{c}(5)=[0110]\} \quad (1)$$

is shown. In the following we denote the set of all N_s trellis states as $\mathcal{S} = \{s_0, \dots, s_{N_s-1}\}$ where the s_k , $k = 0, \dots, N_s - 1$, represent the individual state hypotheses. Furthermore, the bit position for the root state is denoted with ν , $\nu \in \{1, \dots, N\}$, and for the sake of brevity its hypothesis $S_\nu = s_0$ is written as $S_\nu = 0$ in the remainder of this paper.

Due to the unique relationship between VLC tree and VLC trellis every non-leaf or non-root state $S_n = \sigma$, $\sigma \in \mathcal{S} \setminus s_0$, is associated with a certain codeword prefix written as $\mathbf{c}_{[0 \dots \sigma]}$, or equivalently, with a state sequence $[S_\nu, \dots, S_n] = [0, \dots, \sigma]$. This corresponds to a certain subset of codewords $\mathcal{P}_\sigma = \{\lambda \in \mathcal{I} \mid S_n = \sigma \in \mathbf{c}(\lambda), \sigma \in \mathcal{S} \setminus s_0\}$ with the common prefix $\mathbf{c}_{[0 \dots \sigma]}$.

2.3. A-posteriori probabilities

Based on the VLC trellis representation from above we now derive a soft-input decoding algorithm, which provides reliability information for the source bits $b_n = i$, $i \in \{0, 1\}$, in form of a-posteriori probabilities (APPs) $P(b_n = i | \hat{\mathbf{b}})$. As a new result we show that it is possible to exploit the first-order Markov property of the quantization indices modeled

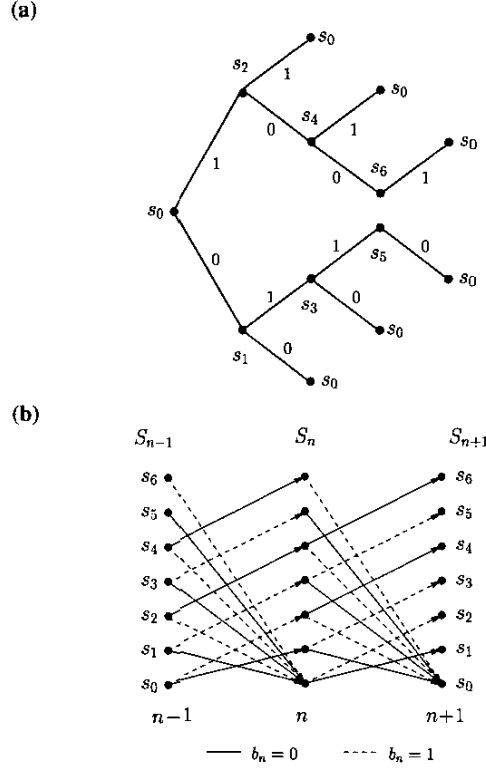


Fig. 2. (a) Code tree and (b) trellis representation for the RVLC codetable in (1)

by the index transition probabilities $P(I_k = \lambda \mid I_{k-1} = \mu)$ as a-priori information in the bit-based decoding algorithm.

Analog to the classical BCJR algorithm [2] the APPs $P(b_n = i | \hat{\mathbf{b}})$ can be decomposed as

$$P(b_n = i | \hat{\mathbf{b}}) = \frac{1}{p(\hat{\mathbf{b}})} \sum_{\sigma_1 \in \mathcal{S}} \sum_{\sigma_2 \in \mathcal{S}} \underbrace{p(\hat{\mathbf{b}}_{n+1}^N | S_n = \sigma_2)}_{\beta_n(\sigma_2)} \cdot \underbrace{p(\hat{b}_n, b_n = i, S_n = \sigma_2 | S_{n-1} = \sigma_1, \hat{\mathbf{b}}_1^{n-1})}_{\gamma_n(i, \sigma_2, \sigma_1)} \cdot \underbrace{p(\hat{\mathbf{b}}_1^{n-1}, S_{n-1} = \sigma_1)}_{\alpha_{n-1}(\sigma_1)}, \quad (2)$$

where $\hat{\mathbf{b}}_{n_1}^{n_2}$ specifies the subsequence $\hat{\mathbf{b}}_{n_1}^{n_2} = [\hat{b}_{n_1}, \hat{b}_{n_1+1}, \dots, \hat{b}_{n_2}]$. The term $\alpha_n(\sigma_2)$ represents the well-known BCJR forward recursion

$$\alpha_n(\sigma_2) = \sum_{\sigma_1 \in \mathcal{S}} \sum_{i=0}^1 \gamma_n(i, \sigma_2, \sigma_1) \alpha_{n-1}(\sigma_1), \quad \alpha_0(0) = 1, \quad (3)$$

with $\gamma_n(i, \sigma_2, \sigma_1) = p(\hat{b}_n | b_n = i)$.

$$P(b_n = i, S_n = \sigma_2 | S_{n-1} = \sigma_1, \hat{\mathbf{b}}_1^{n-1}). \quad (4)$$

The first term on the right-hand side of (4) corresponds to the soft output of the transmission channel associated with the bit $b_n = i$. The second term specifies the probability of a transition from state $S_{n-1} = \sigma_1$ to state $S_n = \sigma_2$ and also depends on the previously received soft-bits $\hat{\mathbf{b}}_1^{n-1}$, which allows to include the statistics of the Markov source model into the decoding process as we will show in the following.

We start the derivation by formally extending the conditional p.d.f. $\gamma_n(i, \sigma_2, \sigma_1)$ in (2) to the whole codeword prefix given by the transition from the previous root state $S_\nu = 0$ to $S_n = \sigma_2$:

$$p(\hat{\mathbf{b}}_{\nu+1}^n, \mathbf{c}_{[0\dots\sigma_2]} | S_\nu = 0, \hat{\mathbf{b}}_1^\nu) = p(\hat{\mathbf{b}}_{\nu+1}^n | \mathbf{c}_{[0\dots\sigma_2]}) \cdot P(\mathbf{c}_{[0\dots\sigma_2]} | S_\nu = 0, \hat{\mathbf{b}}_1^\nu), \quad (5)$$

where the bit position $\nu = n - l(\mathbf{c}_{[0\dots\sigma_2]})$ corresponds to the root state of the path associated with the prefix $\mathbf{c}_{[0\dots\sigma_2]}$ in the VLC code tree. When we now use the fact that the a-priori probability for $\mathbf{c}_{[0\dots\sigma_2]}$ is equivalent to the sum of the a-priori probabilities for the affected source indices we obtain

$$P(\mathbf{c}_{[0\dots\sigma_2]} | S_\nu = 0, \hat{\mathbf{b}}_1^\nu) = \sum_{\lambda \in \mathcal{P}_{\sigma_2}} P(I_0 = \lambda | S_\nu = 0, \hat{\mathbf{b}}_1^\nu) \quad (6)$$

with $P(I_0 = \lambda | S_\nu = 0, \hat{\mathbf{b}}_1^\nu)$ denoting the conditional probability of the source hypothesis $I_0 = \lambda$. For the sake of clarity the source indices I_k are referenced relatively to the currently considered trellis path segment from bit position ν to $\nu + l(\mathbf{c}(\lambda))$ (which corresponds to $k=0$).

It can now be shown that by combining (4), (5), and (6) the second term on the right-hand side of (4) can be written as a function of index-based conditional probabilities according to

$$P(b_n = i, S_n = \sigma_2 | S_{n-1} = \sigma_1, \hat{\mathbf{b}}_1^{n-1}) = \frac{1}{C(\sigma_1)} \sum_{\lambda \in \mathcal{P}_{\sigma_2}} P(I_0 = \lambda | S_\nu = 0, \hat{\mathbf{b}}_1^\nu) \quad (7)$$

with the normalization factor $C(\sigma_1)$. Since $P(I_0 = \lambda | S_\nu = 0, \hat{\mathbf{b}}_1^\nu)$ in (7) can be written as

$$P(I_0 = \lambda | S_\nu = 0, \hat{\mathbf{b}}_1^\nu) = \sum_{\mu=0}^{2^M-1} P(I_0 = \lambda | I_{-1} = \mu) \cdot P(I_{-1} = \mu | S_\nu = 0, \hat{\mathbf{b}}_1^\nu) \quad (8)$$

we can now utilize the index transition probabilities $P(I_0 = \lambda | I_{-1} = \mu)$ as a-priori information for APP decoding. The last missing term to be expressed with known quantities is the conditional probability $P(I_{-1} = \mu | S_\nu = 0, \hat{\mathbf{b}}_1^\nu)$ in (8). Due to the fact that the trellis branch specified by the triple $(S_{\nu-1} = \sigma_0, S_\nu = 0, b_\nu = i)$,

$\sigma_0 \in \mathcal{S}$, uniquely identifies the trellis path associated with the source index $I_{-1} = \mu \in \mathcal{I}$ at the *previous* index position, the hypothesis $I_{-1} = \mu$ may be replaced with $b_\nu = i(\mu)$ and $S_{\nu-1} = \sigma_0(\mu)$ which now depend on μ . We thus obtain the recursion

$$\begin{aligned} P(I_{-1} = \mu | S_\nu = 0, \hat{\mathbf{b}}_1^\nu) &= P(b_\nu = i(\mu), S_{\nu-1} = \sigma_0(\mu) | S_\nu = 0, \hat{\mathbf{b}}_1^\nu) \\ &= \frac{1}{\alpha_\nu(0)} \cdot \gamma_\nu(i(\mu), 0, \sigma_0(\mu)) \cdot \alpha_{\nu-1}(\sigma_0(\mu)), \quad (9) \end{aligned}$$

where the term $\alpha_\nu(0)$ is a normalization factor only depending on the bit position ν for the root state. Finally, combining (4), (7), (8), and (9) leads to a modified expression for the γ -term which allows us to exploit the residual source correlation for error resilience in the forward recursion (3).

The β -term in (2) can be obtained analog to the backward recursion of the BCJR algorithm as

$$\beta_n(\sigma_1) = \sum_{\sigma_2 \in \mathcal{S}} \sum_{i=0}^1 \gamma'_{n+1}(i, \sigma_2, \sigma_1) \cdot \beta_{n+1}(\sigma_2), \quad \beta_N(0) = 1. \quad (10)$$

Again, the γ' -term considers the a-priori knowledge of the source and the transition model and by using similar arguments as for the α -term we obtain

$$\gamma'_n(i, \sigma_2, \sigma_1) = \frac{p(\hat{b}_n | b_n = i)}{C'(\sigma_1)} \cdot \sum_{\lambda \in \mathcal{P}_{\sigma_2}} P(I_0 = \lambda), \quad (11)$$

where $C'(\sigma_1)$ is some normalization factor. Note that for the backward recursion only the probability distribution $P(I_k = \lambda)$ can be utilized as additional a-priori information since at the root state $S_\nu = 0$ no further knowledge about the source indices I_ℓ for $\ell < 0$ is available.

Now we have derived all terms in order to calculate the APPs $P(b_n = i | \hat{\mathbf{b}})$ from (2) with known quantities, where besides the source statistics only the number of transmitted bits N is used as side information in the APP calculation. Finally, a source symbol packet estimate $\hat{\mathbf{U}}$ can be obtained via a MAP sequence estimation (see e.g. [9]) where the bit-based APPs $P(b_n = i | \hat{\mathbf{b}})$ are used to calculate the corresponding path metrics.

3. ITERATIVE DECODING AND EXIT CHARTS

In the following we additionally consider explicit redundancy from channel codes inserted into the interleaved output of the VLC encoder, which leads to the extended transmission system shown in Fig. 3. Since the encoder configuration is similar to that for serially concatenated codes, the decoding can be carried out iteratively, where the outer constituent decoder is replaced by the APP VLC source decoder derived in Section 2.3. Based on an EXIT chart analysis we optimize a rate-1 channel code for a given VLC in order to obtain good convergence properties for the iterative decoder.

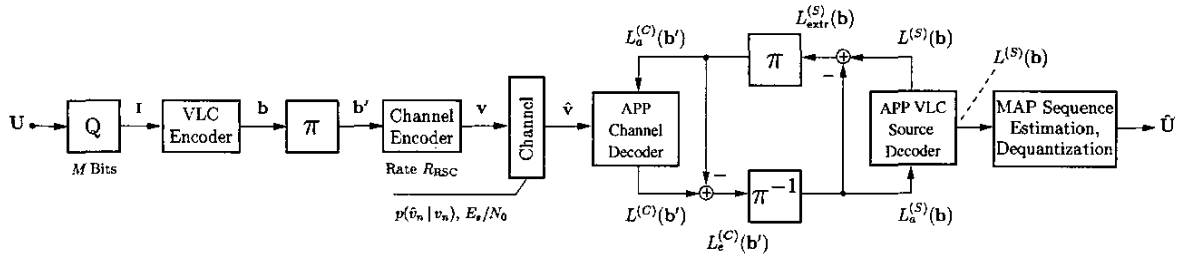


Fig. 3. Extended model of the transmission system and iterative joint source-channel decoder

3.1. Iterative joint source-channel decoding

Due to the serial concatenation of source and channel encoding the iterative decoder depicted in Fig. 3 can be used for calculating a-posteriori probabilities for the decoded information bits. In the decoding process the (inner) APP channel decoder calculates a-posteriori log-likelihood-ratios (LLRs) $L^{(C)}(\mathbf{b}')$ for the interleaved information bit vector $\mathbf{b}' = [b'_1, b'_2, \dots, b'_N]$. The quantity $L_e^{(C)}(\mathbf{b}') = L^{(C)}(\mathbf{b}') - L_a^{(C)}(\mathbf{b}')$ is used after deinterleaving by the (outer) APP source decoder as a-priori information $L_a^{(S)}(\mathbf{b})$ in order to obtain the a-posteriori LLRs $L^{(S)}(\mathbf{b})$. For completing the iteration the APP source decoder generates the extrinsic information $L_{\text{extr}}^{(S)}(\mathbf{b}) = L^{(S)}(\mathbf{b}) - L_a^{(S)}(\mathbf{b})$ which after interleaving can be exploited as additional a-priori information $L_a^{(C)}(\mathbf{b}')$ by the inner decoder at the beginning of the next iteration. Finally, a MAP sequence estimation is performed on the LLRs $L^{(S)}(\mathbf{b})$ in order to obtain an estimate $\hat{\mathbf{U}}$ of the transmitted source sequence \mathbf{U} .

3.2. EXIT charts

In order to analyze the iterative decoding process we apply an EXIT chart analysis [7] to the problem of iterative joint source-channel decoding. EXIT charts visualize the input/output characteristics of the constituent decoders in terms of mutual information between transmitted bit sequence \mathbf{b} and a-priori information $L_a(\mathbf{b})$ at the input of the decoder, and between \mathbf{b} and $L_e(\mathbf{b})$ at the output, respectively. Denoting the mutual information I at the inputs/outputs of the inner and outer decoder as

$$I_{E_i} = I(L_e^{(C)}(\mathbf{b}'), \mathbf{b}') \quad \text{and} \quad I_{A_i} = I(L_a^{(C)}(\mathbf{b}'), \mathbf{b}'),$$

$$I_{E_o} = I(L_{\text{extr}}^{(S)}(\mathbf{b}), \mathbf{b}) \quad \text{and} \quad I_{A_o} = I(L_a^{(S)}(\mathbf{b}), \mathbf{b}),$$

the transfer characteristics of the constituent decoders are given by $I_{E_i} = T_i(I_{A_i}, E_s/N_0)$ and $I_{E_o} = T_o(I_{A_o})$, respectively. The function T_i for the inner decoder is parameterized with the channel signal-to-noise ratio (SNR) E_s/N_0 since a-priori information *and* channel observation $\hat{\mathbf{v}}$ are employed in the decoding process, while the transfer characteristics T_o of the outer constituent decoder only depends on I_{A_o} . An EXIT chart can be obtained by plotting both mappings T_i and T_o into a single diagram.

In the following we propose a transmission system where some explicit redundancy for error protection is also added in the VLC encoder by using a symmetrical reversible VLC (RVLC) with free distance $d_f = 2$ [10]. Since the channel code still can be arbitrarily chosen, good codes in terms of convergence behavior and decoding performance may be searched via an EXIT chart analysis. In this connection we restrict ourselves to rate-1 channel codes, which do not introduce further (explicit) redundancy into the variable-length encoded bitstream. Fig. 4 shows the EXIT chart of the resulting iterative joint source-channel decoder. The transfer characteristic $T_o(I_{A_o})$ of the (outer) RVLC source decoder is derived for an AR(1) input process with correlation coefficient $\alpha = 0.9$, uniformly quantized with $M = 4$ bits. The mapping $T_i(I_{A_i}, E_s/N_0)$ is obtained for a rate-1 recursive systematic convolutional (RSC) channel code being punctured from a rate-1/2 memory-3 mother code with generator polynomials $(g_0, g_1)_8 = (15, 10)_8$, where the puncturing pattern $\mathbf{P} = [1, 0, 0; 0, 1, 1]$ is obtained from the EXIT-chart-based code search. In order to illustrate the it-

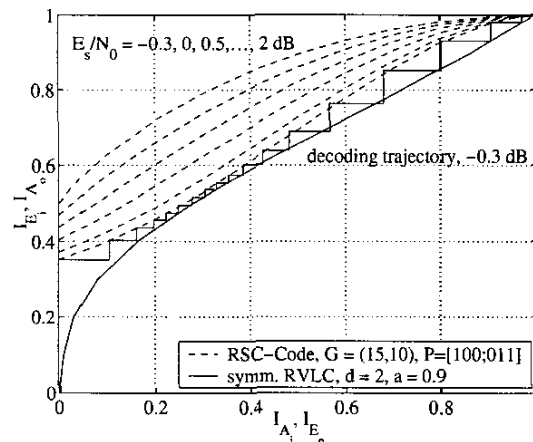


Fig. 4. EXIT chart for the iterative source-channel decoder

erative decoding process Fig. 4 also depicts a simulated decoding trajectory for $E_s/N_0 = -0.3$ dB. We can see that the decoder is able to pass the bottleneck region, thus guaranteeing convergence for this channel SNR.

4. SIMULATION RESULTS

In order to verify the performance of the resulting transmission system for the constituent codes from Section 3.2 simulations were carried out for a BPSK-modulated AWGN channel and a correlated quantized AR(1) source ($a = 0.9$, $M = 4$) of 20000 source symbols. Fig. 5 shows the symbol error rate (SER) plotted over the channel parameter E_s/N_0 . Additionally, the channel SNR E_b/N_0 related to the transmit energy per information bit $E_b = E_s/R$ is shown with R denoting the overall code rate, which is obtained as $R = R_{RSC} \cdot H(I_k = \lambda | I_{k-1} = \mu) / \bar{M}_{RVLC}$. Note that R contains all redundancy exploited for error protection where the conditional entropy $H(I_k = \lambda | I_{k-1} = \mu)$ takes the redundancy due to the residual source correlation into account and the mean word length after RVLC encoding \bar{M}_{RVLC} the explicit redundancy from the RVLC, respectively. Due to a rate-1 channel code we have $R_{RSC} = 1$, leading to $R = 0.57$ for the here used AR(1) source sequence and the RVLC, respectively. The simulation results for the iterative joint source-channel decoder in Fig. 5 are obtained by averaging over 100 simulated transmissions on the AWGN channel. As we can see from Fig. 5, for 20 iterations and channel

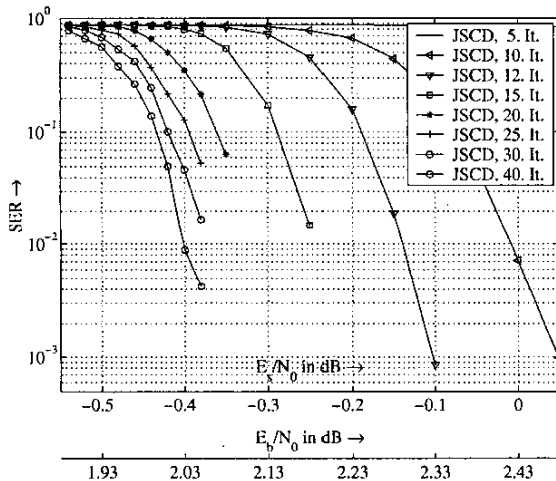


Fig. 5. Simulation results for the AWGN channel, symbol error rate (SER) displayed over E_s/N_0 and E_b/N_0 , resp. (AR(1) source with $a = 0.9$ and $M = 4$, RVLC with $d_f = 2$, rate-1 memory-3 RSC code, overall code rate $R = 0.57$)

SNRs $E_s/N_0 \geq -0.3$ dB and $E_b/N_0 \geq 2.13$ dB, resp., a reliable transmission is possible since no error event occurs. This is consistent with the decoding trajectory for $E_s/N_0 \geq -0.3$ dB shown in Fig. 4 where convergence is achieved after 18 iteration steps.

5. CONCLUSION

We have presented a novel VLC APP decoding approach which can be regarded as an extension of the classical

bit-based BCJR algorithm adapted to the case of variable-length encoded first-order Markov sources. Its advantage is the combination of symbol-based source statistics used as a priori information for robust source decoding and a simple bit-level trellis representation. This leads to a significant reduction of complexity compared to previous work due to the strongly reduced number of trellis states especially for long packets of source data. When an additional error protection by channel codes is performed the proposed VLC APP decoder can be used as (outer) constituent decoder in an iterative joint source-channel decoding scheme. An EXIT-chart-based analysis reveals that by using RVLCs with distance constraints a reliable transmission with rate-1 convolutional codes is possible even at low SNR on the transmission channel. This may justify a new source-channel encoding paradigm where explicit redundancy for error protection is exclusively being added only in the source encoding stage.

6. REFERENCES

- [1] R. Bauer and J. Hagenauer, "Symbol-by-symbol MAP decoding of variable length codes," in *Proc. 3. ITG Conf. on Source and Channel Coding*, Munich, Germany, Jan. 2000, pp. 111–116.
- [2] L. R. Bahl, J. Cocke, F. Jelinek, and J. Raviv, "Optimal decoding of linear codes for minimizing symbol error rate," *IEEE Trans. on Inf. Theory*, pp. 294–287, Mar. 1974.
- [3] J. Klierer and R. Thobaben, "Combining FEC and optimal soft-input source decoding for the reliable transmission of correlated variable-length encoded signals," in *Proc. IEEE Data Compression Conference*, Snowbird, UT, USA, Apr. 2002, pp. 83–91.
- [4] V. B. Balakirsky, "Joint source-channel coding with variable length codes," in *Proc. IEEE Int. Sympos. Information Theory*, Ulm, Germany, June 1997, p. 419.
- [5] R. Bauer and J. Hagenauer, "On variable length codes for iterative source/channel decoding," in *Proc. IEEE Data Compression Conference*, Snowbird, UT, USA, Mar. 2001, pp. 273–282.
- [6] K. Laković and J. Villasenor, "Combining variable length codes and turbo codes," in *Proc. IEEE 55th Vehicular Technology Conference*, Birmingham, AL, USA, May 2002, pp. 1719–1723.
- [7] S. ten Brink, "Code characteristic matching for iterative decoding of serially concatenated codes," *Annals of Telecommunications*, vol. 56, no. 7-8, pp. 394–408, July-August 2001.
- [8] Y. Takishima, M. Wada, and H. Murakami, "Reversible variable length codes," *IEEE Trans. on Comm.*, vol. 43, no. 2/3/4, pp. 158–162, Feb./Mar./April 1995.
- [9] M. Park and D. J. Miller, "Joint source-channel decoding for variable-length encoded data by exact and approximate MAP sequence estimation," *IEEE Trans. on Comm.*, vol. 48, no. 1, pp. 1–6, Jan. 2000.
- [10] K. Laković and J. Villasenor, "On design of error-correcting reversible variable length codes," *IEEE Communications Letters*, vol. 6, no. 8, pp. 337–340, Aug. 2002.